

# Electron correlation and spin density wave order in iron pnictides

Sen Zhou<sup>1</sup> and Ziqiang Wang<sup>2</sup>

<sup>1</sup> *National High Magnetic Field Laboratory, Florida State University, Tallahassee, Florida 32310, USA and*

<sup>2</sup> *Department of Physics, Boston College, Chestnut Hill, Massachusetts 02467, USA*

(Dated: February 22, 2024)

We study the correlation effects on the electronic structure and spin density wave order in Fe-pnictides. Using the multiorbital Hubbard model and Gutzwiller projection, we show that correlation effects are essential to stabilize the metallic spin density wave phase for the intermediate correlation strengths appropriate for pnictides. We find that the ordered moments depend sensitively on the Hund's rule coupling  $J$  but weakly on the intraorbital Coulomb repulsion  $U$ , varying from  $0.3\mu_B$  to  $1.5\mu_B$  in the range  $J = 0.3 \sim 0.8$  eV for  $U = 3 \sim 4$  eV. We obtain the phase diagram and discuss the effects of orbital order and electron doping, the evolution of the Fermi surface topology with the ordered moment, and compare to recent experiments.

PACS numbers: 71.27.+a, 74.70.Xa, 74.25.Ha, 74.25.Jb

The iron pnictides have emerged recently as another class of high- $T_c$  superconductors [1] involving the transition metal  $d$ -electrons in addition to the cuprates. In the two most studied pnictide families, the 1111 (e.g.  $\text{LaO}_{1-x}\text{F}_x\text{FeAs}$ ) and the 122 series (e.g.  $\text{Ba}_{1-x}\text{K}_x\text{Fe}_2\text{As}_2$ ), the iron valence is  $\text{Fe}^{2+}$ . There are six electrons occupying five Fe  $3d$  orbitals. Their direct overlap and via As  $4p$  orbitals produce five energy bands with a total bandwidth around 4eV [2–4]. This is comparable to the on-site Coulomb repulsion  $U = 3 \sim 4$  eV [4] typical for transition metals. Thus, the Fe-pnictides are multiorbital systems where the correlation strength is intermediate and comparable to the kinetic energy. In this intermediate correlation regime lies the challenge of the many-body physics responsible for unconventional electronic ground states and emergent phenomena in condensed matter and complex materials.

That the correlation effects play an important role in pnictides can be seen from the fact that despite of the orbital degeneracy, the normal state behaves quite incoherently with an enhanced magnetic susceptibility in contrast to conventional Fermi liquids [5]. At low temperatures, the observed quasiparticle dispersion [6, 7] exhibits a strong bandwidth reduction due to electron correlations, as shown in a first principle calculation that includes the interaction effects in the Gutzwiller approach [8]. Appropriate treatment of the electron correlation in this intermediate regime, especially its multiorbital nature, is essential for understanding the properties, including the high- $T_c$  superconductivity, of these materials.

In this paper, we investigate the correlation effects on the spin density wave (SDW) order from which the high- $T_c$  superconductivity emerges with sufficient doping. At low temperatures, semi-metallic SDW order develops in the undoped pnictides with an ordering vector  $\mathbf{Q} = (\pi, 0)$  connecting the geometric centers of the electron and hole Fermi surface (FS) pockets in the unfolded Brillouin zone (BZ) containing one Fe atom per unit cell [9, 10]. The atomic states for  $\text{Fe}^{2+}$  is predominantly

$S = 2$  and  $S = 1$  in the presence of Hund's rule coupling and crystal field splitting. However, the ordered Fe moments are much smaller than in the local spin density approximation (LSDA)[11] and vary substantially from mostly about  $0.35\mu_B$  in the 1111 series [9] to around  $1\mu_B$  in the 122 series [10]. This unconventional SDW phase evades the well established theories and appears to straddle the limits of localized and itinerant magnetism.

We show that these unusual properties arise in the immediate correlation regime, provided that the correlation effects are treated appropriately. To this end, we study a multiorbital Hubbard model for the Fe  $t_{2g}$  complex with the hopping parameters determined from the LDA band structure. The intra and interorbital Coulomb repulsion  $U$  and  $U'$ , and the Hund's rule coupling  $J$  are treated by Gutzwiller projection of multi-occupancy in the intermediate correlation regime appropriate for the pnictides. We show that the interplay between correlation and itineracy stabilizes the metallic SDW phase. We found that  $U$  and  $J$  play different roles in controlling the SDW order and the bandwidth reduction. The ordered moments depend sensitively on Hund's rule coupling but weakly on  $U$  and varies from  $0.3\mu_B$  to  $1.5\mu_B$  in the range  $J = 0.3 \sim 0.8$  eV and  $U = 3 \sim 4$  eV consistent with experimental observations. The phase diagram is obtained in the parameter space of  $U$  and  $J$  and contrasted to the perturbative Hartree-Fock (HF) theory that erroneously predicts a SDW metal-insulator transition (MIT). We elucidate the interplay between the crystal field renormalization and the magnetization induced band splitting and discuss the multiorbital nature of the SDW and orbital order. The band dispersions and the FS topology are shown to vary significantly as a function of the SDW moment with implications for the ARPES experiments. We also present results for the destruction of the SDW order with electron doping.

The Hamiltonian is written as  $\hat{\mathcal{H}} = \hat{\mathcal{H}}_0 + \hat{\mathcal{H}}_I$  where

$$\hat{\mathcal{H}}_0 = \sum_{ij, \alpha\beta, \sigma} t_{\alpha\beta} [x_j - x_i, y_j - y_i] c_{i\alpha\sigma}^\dagger c_{j\beta\sigma} + \sum_{i, \alpha} \Delta_\alpha^0 \hat{n}_{i\alpha}, \quad (1)$$

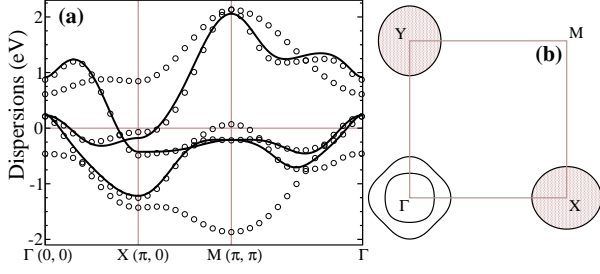


FIG. 1: *Three-band tight-binding model.* (a) Band dispersions (lines) and (b) Fermi surfaces. Open circles in (a) denote the dispersions of the five-band model of Ref. [3].

describes the band structure of the Fe 3d complex that dominates the low energy density of states in LDA [3, 4]. Here  $c_{i\alpha\sigma}^\dagger$  creates an electron in orbital  $\alpha$  with spin  $\sigma$  on site  $i$ ,  $\hat{n}_{i\alpha}$  is the density operator and  $\Delta_\alpha^0$  is the crystal field splitting. Since the dispersions near the Fermi energy and the FS topology can be captured by three  $t_{2g}$  orbitals [12, 13], we work with a three-orbital model with  $\alpha, \beta=1$  ( $d_{xz}$ ), 2 ( $d_{yz}$ ), 3 ( $d_{xy}$ ) derived from the five-band model of Kuroki *et al.* for the LDA band dispersions of LaOFeAs [3]. The corresponding hopping integrals  $t_{\alpha\beta}[x_j - x_i, y_j - y_i]$  are given in Table I and  $\Delta_\alpha^0 = \{0, 0, \Delta_0 = 0.16\text{eV}\}$ . The dispersion and FSs are shown in Fig. 1 for the undoped case with four electrons per Fe site. There are two hole pockets centered around  $\Gamma$  and two electron pockets around  $X$  and  $Y$  in the unfolded BZ. Note that although the joint density of states is enhanced, there is no FS nesting by the vector  $\mathbf{Q}$  and our results are not sensitive to the details of the band parameters and the shape of the FSs.

TABLE I: Hopping integrals  $t_{\alpha\beta}[\Delta x, \Delta y]$  up to five neighbors in unit of meV. Notations are the same as in Ref. [3].

$(\alpha, \beta)$	[1, 0]	[1, 1]	[2, 0]	[2, 1]	[2, 2]	$\mathbf{I}$	$\sigma_d$	$\sigma_y$
(1,1)	54.1	39.1	-89.2	16.2	3.3	+	+	+(2,2)
(2,2)	41.6	39.1	38.9	-8.4	3.3	+	+	+(1,1)
(3,3)	-109.7	337.9	14.3	-16.4	-6.1	+	+	+
(1,2)	0	122.5	0	22.9	-0.5	+	-	+
(1,3)	-346.3	-26.1	10.5	-4.8	-11.6	-	+	-(2,3)
(2,3)	0	26.1	0	22.4	11.6	-	-	-(1,3)

The multi-orbital local correlations are described by

$$\hat{\mathcal{H}}_I = U \sum_{i,\alpha} \hat{n}_{i\alpha\uparrow} \hat{n}_{i\alpha\downarrow} + \left( U' - \frac{1}{2}J \right) \sum_{i,\alpha<\beta} \hat{n}_{i\alpha} \hat{n}_{i\beta} \quad (2)$$

$$- J \sum_{i,\alpha \neq \beta} \mathbf{S}_{i\alpha} \cdot \mathbf{S}_{i\beta} + J \sum_{i,\alpha \neq \beta} c_{i\alpha\uparrow}^\dagger c_{i\alpha\downarrow}^\dagger c_{i\beta\downarrow} c_{i\beta\uparrow},$$

with  $U = U' + 2J$ . In the perturbative treatment, the interactions are decoupled in the HF approximation,

$$\langle c_{i\alpha\sigma}^\dagger c_{i\beta\sigma'} \rangle = \frac{1}{2} [n_\alpha + \sigma m_\alpha \cos(\mathbf{Q} \cdot \mathbf{r}_i)] \delta_{\alpha\beta} \delta_{\sigma\sigma'},$$

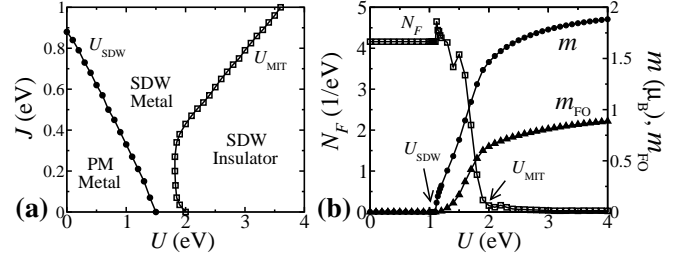


FIG. 2: *HF results.* (a) Phase diagrams on the  $U$ - $J$  plane. (b) Magnetization  $m$ , FO order  $m_{FO}$ , and the Fermi level DOS  $N_F$  as a function of  $U$  along the trajectory  $U = 5J$ .

where  $n_\alpha$  and  $m_\alpha$  the charge density and magnetization on orbital  $\alpha$ . They are determined self-consistently in the internal orbital-dependent fields in the charge and spin sector respectively:  $\Delta_\alpha = \frac{1}{2}(2U - 5J)n - \frac{1}{2}(U - 5J)n_\alpha$ ,  $h_\alpha = \frac{1}{2}Jm + \frac{1}{2}(U - J)m_\alpha$ . Clearly,  $\Delta_\alpha$  renormalizes the crystal field splitting and governs the orbital carrier transfer [14] while  $h_\alpha$  controls the distribution of the magnetic moment over the three orbitals. The HF phase diagram is shown in Fig. 2a on the  $U$ - $J$  plane. There are two phase boundaries,  $U_{SDW}$  and  $U_{MIT}$ , separating the paramagnetic (PM) phase, the  $\mathbf{Q}$ -SDW metal, and the  $\mathbf{Q}$ -SDW insulator, respectively. The evolutions of the magnetization  $m = \sum_\alpha m_\alpha$ , the density of states (DOS) at the Fermi level  $N_F$ , and the ferro-orbital (FO) order  $m_{FO} = n_{yz} - n_{xz}$  that lifts the degeneracy between  $d_{xz}$  and  $d_{yz}$  [15] are shown in Fig. 2b as a function of the correlation strength along the trajectory  $U = 5J$ . Due to the absence of FS nesting, the PM state is stable until  $U_{SDW} \sim 1.1$  eV where SDW and FO order develop simultaneously, followed by a MIT at  $U_{MIT} \sim 1.9$  eV beyond which all FS pockets are fully gapped. The origin of the insulating SDW phase is worth noting. The SDW order is usually tied to the gapping of the band crossings (nodes) upon folding by the ordering vector  $\mathbf{Q}$ . However, the symmetry and topology of the orbitals in the FeAs plane require that the nodes be annihilated in sets of four [16]. The six nodes in the LDA band structure of LaOFeAs near  $E_F$  implies a gapless SDW state [16]. We find that additional nodes are created in pairs as the magnetization increases. The subsequent nodal annihilation in sets of four produces a fully gapped SDW state. Indeed, for  $U = 3 \sim 4$  eV and  $J = 0.3 \sim 0.8$  eV appropriate for the Fe-pnictides, the perturbative HF theory would predict an insulating SDW state with large magnetization (also found in [17]), contradicting experimental observations. This is rooted in the fact that the HF self-energies, i.e. the internal fields  $\Delta_\alpha$  and  $h_\alpha$  scale with the correlation strengths due to multioccupation and fail to capture correctly the correlation effects.

To treat interactions appropriately, it is necessary to take into account that the probabilities for multi-occupation of the atomic orbitals are energetically costly and significantly reduced even for intermediate correlations. Since the  $\mathbf{Q}$ -SDW is collinear, it is sufficient

to focus on the spin-dependent density-density interactions in Eq. (2). The atomic multiplets are thus the  $4^M$  ( $M = 3$  is the number of orbitals) local Fock states  $|\Gamma\rangle = \prod_{\alpha\sigma} (c_{\alpha\sigma}^\dagger)^{n_{\alpha\sigma}} |0\rangle$ , where  $n_{\alpha\sigma}^\Gamma = \langle \Gamma | \hat{n}_{\alpha\sigma} | \Gamma \rangle = 0$  or 1. The ground state can be obtained by Gutzwiller projected wave function  $|\Psi_G\rangle = \hat{P}_G |\Psi_0\rangle$ , where  $|\Psi_0\rangle$  is a Slater determinate state and  $\hat{P}_G$  is the projection operator that reduces the probability of multi-occupancy states in  $|\Gamma\rangle$ . The multiorbital Gutzwiller projection [18] can be formulated in the grand canonical ensemble,

$$\hat{P}_G = \prod_i \hat{P}_i, \quad \hat{P}_i = \sum_{\Gamma} \left( \prod_{\alpha\sigma} y_{i\alpha\sigma}^{n_{\alpha\sigma}^\Gamma} \right) \eta_{i\Gamma} \hat{m}_{i\Gamma}, \quad (3)$$

where  $\hat{m}_{i\Gamma} = |i\Gamma\rangle\langle i\Gamma| = \prod_{\alpha\sigma} (\hat{n}_{\alpha\sigma}^\Gamma)^{n_{\alpha\sigma}^\Gamma} (1 - \hat{n}_{\alpha\sigma}^\Gamma)^{1-n_{\alpha\sigma}^\Gamma}$  projects onto the local Fock state  $|i\Gamma\rangle$  and  $\eta_{i\Gamma}$  is the probability weighting factor determined variationally. The density operator  $\hat{n}_{i\alpha\sigma} = \sum_{\Gamma} n_{\alpha\sigma}^\Gamma \hat{m}_{i\Gamma}$ . In Eq. (3), the spin-orbital dependent local fugacities  $y_{i\alpha\sigma}$  maintain the charge density under the projection, i.e.,  $n_{i\alpha\sigma}^0 = n_{i\alpha\sigma} = \sum_{\Gamma} n_{\alpha\sigma}^\Gamma m_{i\Gamma}$ , with  $m_{i\Gamma} = \langle \Psi_G | \hat{m}_{i\Gamma} | \Psi_G \rangle$ . The projection is conveniently implemented using the Gutzwiller approximation (GA) [18] and is taken into account locally by the statistical weighting factor multiplying the quantum coherent state. For the hopping term, we find  $\langle \Psi_G | c_{i\alpha\sigma}^\dagger c_{j\beta\sigma} | \Psi_G \rangle = g_{i\alpha,j\beta}^\sigma \langle \Psi_0 | c_{i\alpha\sigma}^\dagger c_{j\beta\sigma} | \Psi_0 \rangle$ , where the Gutzwiller factor  $g_{i\alpha,j\beta}^\sigma = g_{i\alpha\sigma} g_{j\beta\sigma}$ ,  $g_{i\alpha\sigma} = \langle \Psi_0 | \hat{W}_{i\alpha\sigma} | \Psi_0 \rangle / \langle \Psi_0 | \hat{P}_i^2 | \Psi_0 \rangle$  with  $\hat{W}_{i\alpha\sigma} c_{i\alpha\sigma}^\dagger = \hat{P}_i c_{i\alpha\sigma}^\dagger \hat{P}_i$ ,

$$g_{i\alpha\sigma} = \frac{1}{\sqrt{n_{i\alpha\sigma}^0 (1 - n_{i\alpha\sigma}^0)}} \sum_{\Gamma, \Gamma'} D_{\Gamma\Gamma'}^{\alpha\sigma} \sqrt{m_{i\Gamma} m_{i\Gamma'}}. \quad (4)$$

Here  $D_{\Gamma\Gamma'}^{\alpha\sigma} = \langle \Gamma | c_{i\alpha\sigma}^\dagger | \Gamma' \rangle = 0$  or 1 describes the entanglement between the two multiplets. Hence the projection leads to a nonperturbatively renormalized Hamiltonian,

$$\hat{\mathcal{H}}_{\text{GA}} = \sum_{\mathbf{k}} K_{s'\beta, \mathbf{k}}^{s\alpha, \sigma} c_{s\alpha, \mathbf{k}\sigma}^\dagger c_{s'\beta, \mathbf{k}\sigma} + \tilde{E}_{s\Gamma} m_{s\Gamma} \quad (5)$$

where  $s$  labels the two-sublattice in the **Q**-SDW state, repeated indices are summed, and  $K_{s'\beta, \mathbf{k}}^{s\alpha, \sigma} = g_{s\alpha, s'\beta}^\sigma \varepsilon_{s\alpha, s'\beta}(\mathbf{k}) + (\Delta_\alpha^0 + \epsilon_{s\alpha\sigma}) \delta_{ss'} \delta_{\alpha\beta}$  with  $\mathbf{k}$  in the reduced BZ. The  $\varepsilon_{s\alpha, s'\beta}(\mathbf{k})$  are the LDA band dispersions of  $\hat{\mathcal{H}}_0$ . The main correlation effects are the orbital dependent bandwidth reduction by the Gutzwiller factor; and a renormalization of the crystal field splitting  $\Delta_\alpha^0$  by  $\epsilon_{s\alpha\sigma}$  that originate from the fugacities and scale with the kinetic energy. Note that, in contrast to the HF approximation, there are no internal fields or self-energies proportional to the correlation strengths for the fermionic quasiparticles.  $U$  and  $J$  only appear in the energy level  $E_\Gamma$  of the atomic multiplets  $m_{s\Gamma}$  in Eq. (5) where  $\tilde{E}_{s\Gamma} = E_\Gamma - \sum_{\alpha\sigma} \epsilon_{s\alpha\sigma} n_{\alpha\sigma}^\Gamma$ . The variational parameters  $\{m_{s\Gamma}, \epsilon_{s\alpha\sigma}\}$  are determined self-consistently by minimizing the ground state energy of  $\hat{\mathcal{H}}_{\text{GA}}$  under the completeness condition  $\sum_{\Gamma} \hat{m}_{i\Gamma} = 1$ .

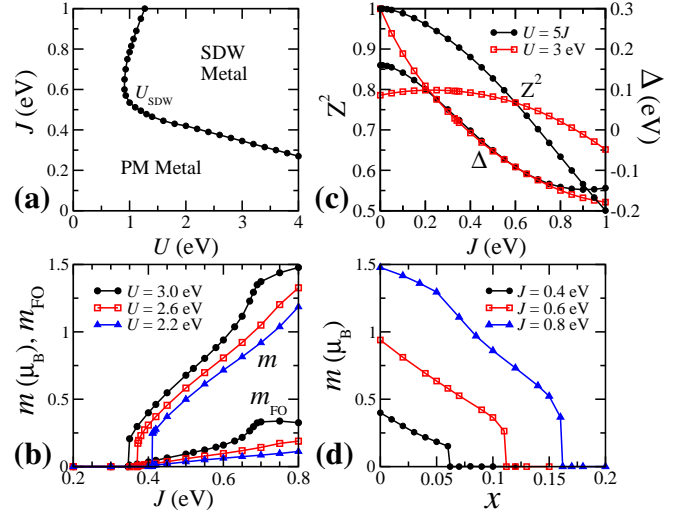


FIG. 3: (color online). *GA results.* (a) Phase diagram. (b) Magnetization  $m$  and FO order  $m_{\text{FO}}$ . (c) band-narrowing factor  $Z^2$  and renormalized crystal field splitting  $\Delta$  as a function of  $J$  at  $U = 3\text{eV}$  and for  $U = 5J$ . (a)-(c) are for undoped case. (d) Electron doping  $x$  dependence of  $m$  at  $U = 3\text{eV}$ .

The nonperturbative phase diagram is shown in Fig. 3a where a metallic **Q**-SDW phase emerges at intermediate values of  $(U, J)$  appropriate for the pnictides. The gaplessness or the metallicity of this phase is stabilized by the correlation effects taken into account nonperturbatively in the Gutzwiller approach. The crystal field renormalization in Eq. (5) counteracts the band splitting due to magnetization. The insulating SDW phase erroneously appeared in the HF theory (Fig. 2a) has a much higher energy and is absent in this regime. The phase boundary has an interesting wedged shape indicating that the transition is predominantly  $J$  driven for intermediate  $U$  and  $U$  driven for large  $J$ . Fig. 3b shows that the ordered moment depends sensitively on the Hund's rule coupling  $J$  and varies from  $0.3\mu_B$  to  $1.5\mu_B$  in the range  $J = 0.3 \sim 0.8\text{eV}$  for a range of intermediate  $U$ . Surprisingly, the ordered moment depends weakly on  $U$  as can be seen from Fig. 3b. This indicates that in the intermediate regime of correlations, the ordered moment is controlled by the increased overlap with the atomic state of higher spins due to the Hund's rule coupling instead of the localization of the carriers due to Coulomb-blocking  $U$ . Note that the orbital order is quite large in the 3-band model shown in Fig. 3b. For  $U = 3\text{eV}$ , the relative orbital polarization  $2m_{\text{FO}}/(n_{xz} + n_{yz})$  ranges from near 8% at  $J = 0.5\text{eV}$  to over 20% near  $J = 0.8\text{eV}$ . It has been shown recently [19] that such significant orbital ordering can partially account for the orthorhombic anisotropy of the reconstructed FS observed by ARPES [20].

The different roles played by  $U$  and  $J$  can also be seen in the PM phase. In Fig. 3c, we plot the average band-narrowing factor  $Z^2 = \frac{1}{M} \sum_{\alpha} g_{\alpha}^2$  [8] and the renormalized crystal field splitting  $\Delta = \Delta_0 + \epsilon_{xy} - \epsilon_{xz, yz}$  as a function of  $J$  for both  $U = 3\text{eV}$  and  $U = 5J$ . The correlation in-

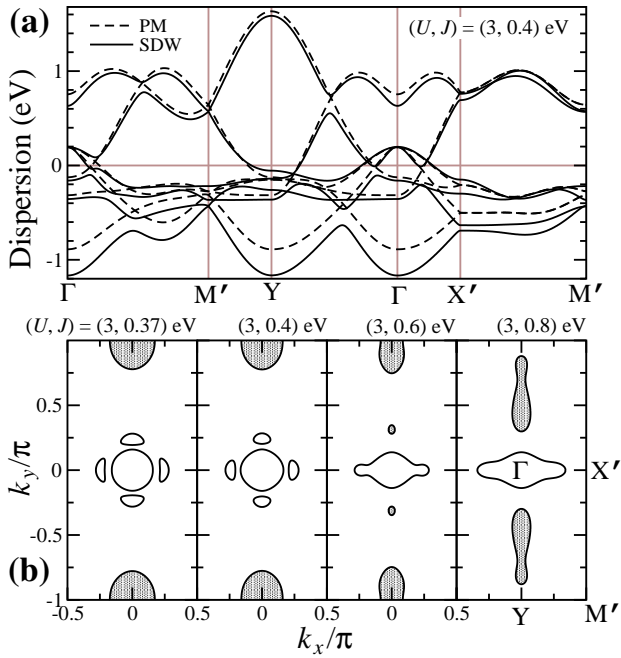


FIG. 4: (a) Band dispersions of the PM and SDW states at  $U = 3$  eV and  $J = 0.4$  eV. (b) FS at four sets of interaction parameters with, from left to right,  $m = 0.3, 0.4, 0.94$ , and  $1.48\mu_B$  respectively. Filled FS pockets are electron-like and open ones are hole-like.

duced bandwidth reduction is predominantly controlled by  $U$  and only weakly depends on  $J$ . The crystal field renormalization is, on the other hand, controlled by the Hund's rule coupling  $J$  and is essentially independent of  $U$  in favor of multiorbital occupation in a wide range of intermediate correlation strengths. Since the intermediate correlation strengths of the pnictides are close to the phase boundary shown in Fig. 3a, applied pressure would increase the wave function overlap and reduce the correlation effects, which may drive the system out of the SDW into the PM phase as observed experimentally [21].

The band dispersions of the PM and SDW states at  $U = 3$  eV and  $J = 0.4$  eV are shown in Fig. 4a. The overall bandwidth is somewhat larger in the SDW phase due to the band splitting by magnetic order. Fig. 4b shows the FS in the SDW state with increasing Hund's rule coupling  $J$  and the corresponding ordered moment. The FS topology are rather sensitive to the magnetization. When the SDW moment is small, the inner hole pocket around  $\Gamma$  and the electron pocket around  $Y$  remains almost unaltered, while the outer hole pocket and the electron pocket around  $X$  suffer strong scattering via  $\mathbf{Q}$ , and become mostly gapped out, leaving behind four small hole pockets around  $\Gamma$  reflecting the Dirac cone-like band crossings. The sizes of the small hole pockets, totaling  $\sim 2\%$  of the reduced BZ, are in reasonable agreement with quantum oscillation experiments on Sr122 and Ba122 [22]. With increasing SDW moment, the two small hole pockets along  $\Gamma$ -X move toward the central hole pocket and eventually disappear as the Dirac

cones are annihilated. The hole pockets along  $\Gamma$ -Y are instead pushed toward the electron FS near  $Y$ , changing character to being electron-like through two Dirac nodes, and eventually coalesce to form one set of elongated electron pockets as shown in Fig. 4b. As a result, the FS topology measured by ARPES [23] would depend rather sensitively on the magnetization in the surface layers.

In summary, we have shown that the multiorbital Hubbard model in the intermediate correlation regime correctly captures the important correlation effects on the electronic structure and the SDW order in the iron-pnictides. A nonperturbative treatment of the interactions is essential to describe this correlated metallic state and the intricate, complementary roles of the Coulomb repulsion and the Hund's rule coupling generic to multiorbital systems. The calculated magnetization is shown in Fig. 3d as a function of the electron doping concentration  $x$  at  $U = 3$  eV for several values of  $J$ . Despite the increase of the spin susceptibility upon doping for our tight binding parameters, the magnetization  $m$  decreases monotonically with electron doping. The results for the case of  $U = 3$  eV and  $J = 0.4$  eV describes well the destruction of SDW order observed experimentally in  $\text{LaO}_{1-x}\text{F}_x\text{FeAs}$ .

We thank Chunhua Li for useful discussions. This work is supported in part by DOE DE-SC0002554, NSF DMR-0704545, and the State of Florida.

- 
- [1] Y. Kamihara *et al.*, J. Am. Chem. Soc. **130**, 3296 (2008); X. H. Chen *et al.*, Nature (London) **453**, 761 (2008); Z.-A. Ren *et al.*, Chin. Phys. Lett. **25**, 2215 (2008); C. Wang *et al.*, Europhys. Lett. **83**, 67006 (2008).
  - [2] D. J. Singh and M. H. Du, Phys. Rev. Lett. **100**, 237003 (2008).
  - [3] K. Kuroki *et al.*, Phys. Rev. Lett. **101**, 087004 (2008).
  - [4] V. I. Anisimov *et al.*, J. Phys: Condens. Matter **21**, 075602 (2009); S. L. Skornyakov *et al.*, Phys. Rev. B **80**, 092501 (2009).
  - [5] K. Haule *et al.*, Phys. Rev. Lett. **100**, 226402 (2008); K. Haule *et al.*, New J. Phys. **11**, 025201 (2009).
  - [6] H. Ding *et al.*, Europhys. Lett. **83**, 47001 (2008); H. Ding *et al.*, arXiv:0812.0534.
  - [7] W. Malaeb *et al.*, J. Phys. Soc. Jpn. **77**, 093714 (2008).
  - [8] G.-T. Wang *et al.*, Phys. Rev. Lett. **104**, 047002 (2010).
  - [9] C. de la Cruz *et al.*, Nature (London) **453**, 899 (2008).
  - [10] J. Zhao *et al.*, Phys. Rev. B **78**, 140504(R) (2008); K. Kaneko *et al.*, Phys. Rev. B **78**, 212502 (2008); Q. Huang *et al.*, Phys. Rev. Lett. **101**, 257003 (2008).
  - [11] C. Cao *et al.*, Phys. Rev. B **77**, 220506(R) (2008); F. Ma and Z.-Y. Lu, Phys. Rev. B **78**, 033111 (2008); Z. P. Yin *et al.*, Phys. Rev. Lett. **101**, 047001 (2008).
  - [12] I. I. Mazin *et al.*, Phys. Rev. Lett. **101**, 057003 (2008).
  - [13] P. A. Lee and X.-G. Wen, Phys. Rev. B **78**, 144517 (2008); M. Daghofer *et al.*, Phys. Rev. B **81**, 014511 (2010).
  - [14] S. Zhou, *et al.*, Phys. Rev. Lett. **94**, 206401 (2005).
  - [15] K. Kubo and P. Thalmeier, J. Phys. Soc. Jpn. **78** 083704 (2009).

- [16] Y. Ran *et al.*, Phys. Rev. B **79**, 014505 (2009).
- [17] R. Yu *et al.*, Phys. Rev. B **79**, 104510 (2009).
- [18] J. Bünemann, W. Weber, and F. Gebhard, Phys. Rev. B **67**, 6898 (1998).
- [19] C.-C. Chen *et al.*, arXiv:1004.4611 (2010).
- [20] T. Shimojima *et al.*, Phys. Rev. Lett. **104**, 057002 (2010).
- [21] B. Lorenz *et al.*, Phys. Rev. B **78**, 012505 (2008).
- [22] S. E. Sebastian *et al.*, J. Phys.: Condens. Matter **20**, 422203 (2008); J. G. Analytis *et al.*, Phys. Rev. B **80**, 064507 (2009).
- [23] D. Hsieh *et al.*, arXiv:0812.2289; G. Liu *et al.*, Phys. Rev. B **80**, 134519 (2009); P. Richard *et al.*, Phys. Rev. Lett. **104**, 137001 (2010).